

The Effect of Brushing on Residual Stress and Surface Roughness of EN AW-2024-T3 Aluminum Alloy Joints Welded Using the FSW Method

Magdalena Bucior^{1*}, Rafał Kluz¹, Andrzej Kubit¹, Kamil Ochał²

¹ Department of Manufacturing Processes and Production Engineering, Rzeszow University of Technology, al. Powstanców Warszawy 8, 35-959 Rzeszów, Poland

² Department of Materials Science, Rzeszow University of Technology, al. Powstanców Warszawy 8, 35-959 Rzeszów, Poland

* Corresponding author's email: magdabucior@prz.edu.pl

ABSTRACT

This article presents the influence of the brushing process on residual stress and surface roughness of EN AW-2024-T3 aluminum alloy joints welded using the Friction Stir Welding (FSW) method. Butt joints with thicknesses of 2 mm were brushed with using ceramic brush. The aim of the study was to find optimal parameters of the brushing process, which would significantly improve the functional properties of welded joints. The experiments were carried out in two steps. In the first stage of the research, the feed rate was changed in the range $f = 40\text{--}120$ mm/min with a constant brushing depth $d = 0.5$ mm. The roughness decreased from $Sa = 5.285$ μm for the specimen after welding to $Sa = 2.460$ μm for the $f = 120$ mm/min and $d = 0.5$ mm. The change in the parameters of the brushing process did not have a significant impact on the state of residual stresses. Hence, in the second step, the brushing depth was increased in steps of 0.1 mm. The best properties were obtained for $f = 120$ mm/min and $d = 0.6$ mm (variant 6A), where roughness was $Sa = 0.443$ μm and compressive stresses $\sigma = -118$ MPa.

Keywords: brushing; aluminum alloy; friction stir welding; surface roughness; residual stress.

INTRODUCTION

Research in the field of friction stir welding (FSW) in recent years has been very popular among scientists and engineers. There is an increasing demand in various industries for development machine parts or structures that are lightweight, durable and cost-effective [1]. This method is successfully used in many industries, including aviation, automotive, shipbuilding, spacecraft or railways [2, 3]. FSW treatment has great potential for joining similar materials such as aluminum [4, 5], copper [6], steel [7] and dissimilar materials such as aluminum and steel [8, 9], aluminium and copper [10, 11] or aluminium and titanium [12]. In the literature, it can be find also tests of welding of dissimilar alloys with different thicknesses [13]. During the process, the frictional

heat generated by the rotating tool causes plastic deformation, which in turn leads to workpiece material mixing and several advantages over conventional joining techniques such as riveting or bolting. For example, the riveting process can be replaced by the FSW process even for the non-weldable aluminum alloys since this process does not include melting and therefore there cannot be any solidification cracking [1]. The unique advantage of this method is that the weld properties can be controlled with only a few process parameters such as feed rate, tool rotation speed, forging pressure and tool tilt angle to achieve the desired weld properties unlike welding which requires multiply process parameters [14].

Despite the numerous advantages of this treatment, there are also problems related to, inter alia, the formation of flashes during the process

(Fig. 2). One of the methods that, in addition to removing flashes, can also reduce surface roughness is brushing with using ceramic brush. The ceramic tool can be used for debburing, barb removal or surface polishing [15]. Tools made of ceramic fibers are an alternative to steel or plastic tools. The disadvantage of steel or plastic tools is the permanent deformation of the fibers, which results in poor surface quality and faster wear.

Many researchers have experimentally used the brushing process for debburing or surface preparation. Author of work [16] used the ceramic brushes for removing burs after Abrasive water – jet machining (AWJM) of EN AW-7075 aluminium alloy. They demonstrated that this treatment reduces surface roughness for all fibre types (White A21, Pink A13, Blue A31 and Red A11) in comparison to surface after AWJM. In turn authors of work [17] used the various ceramic brushed in the debburing operations. They analyzed the effect of various brushing conditions on the axial cutting force in the machining with using the ceramic brush. Authors observed a stronger dependence of the axial force occurring during the brushing process on the spring stiffness compared to the type of brush fibre. Robitaille et al. [18] used brushing process to surface preparation before FSW lap joints. Their study showed that light brushing of Al 2024-T3 AlClad plates, intended to remove the passive oxide scale from the mating surfaces, did not have a significant effect on the microstructural and macrostructural properties of the weld, or on the distribution of the cladding fragments in the joint. The selection of optimal brushing parameters is crucial to enhance the quality of the joints. However, there is on the selection of parameters brushing process for an elements joined with the FSW method.

In this study the effect of brushing treatment on selected mechanical properties such as residual stress and roughness of EN AW-2024-T3 aluminium alloy joints welded with using the FSW method were analyzed. The main aim of this research, to determine the optimal parameters the brushing process with using ceramic brush.

EXPERIMENTAL

Material and methods

In the present study, 2024 aluminum alloy in the T3 temper, with a thickness of 2 mm was

selected to investigate the effect of brushing on residual stress and surface roughness joints welded with FSW method. The chemical composition of the aluminum alloys employed in this paper as follows (in wt.%): Zn (0.25 max), Fe (0.5 max), Ti (0.15 max), Cr (0.1 max), Mg (1.2 ÷ 1.8), Mn (0.3 ÷ 0.9), Cu (3.8 ÷ 4.9), Si (0.5 max) and Al rest [19]. The mechanical properties of EN AW-2024-T3 aluminum as follows: Tensile stress $R_m = 360 \div 425$ MPa, Yield stress $R_e = 250 \div 290$ MPa and Elongation $A = 12 \div 14\%$. This grade of aluminum is especially used in aviation industry for elements of aircraft structures such as: plating of fuselage, wings, control rods, carriers or for the elements of aircraft equipment such as: seat frames, steering columns or covers.

The experimental setup is shown schematically in Figure 1. First, two strips with dimensions $400 \times 100 \times 2$ mm were welded using FSW technology on a universal vertical milling machine Jafo FWF 32J2. The welding process was carried out with the following parameters: rotational speed $n = 1300$ rpm, feed rate $f = 80$ mm/min, depth welding $d = 1.7$ mm, inclination angle of the tool of 3° . The sheets after FSW process with visible burrs was presented in Figure 2a. Next, the brushing process was also performed on a Jafo vertical milling machine. A compensating handle with a spring was attached to the milling head, in which a brush with Xebec White A21 ceramic fibers with a diameter of 15 mm was placed. The Kress spindle used in the tests enables step setting of the rotational speed in the range from 5000 rev/min to 20000 rev/min. In the tests, the brushing speed was 5000 rev/min. Fibre projection length from sleeve was 10 mm, in accordance with the manufacturer's recommendations. The projection length of the fibres was regulated with using an allen screw. The brushing process was carried out on the separate sections of the welded sheet attached to the machine table. In the first stage of the research, the feed speed was changed in the range $f = 40 \div 120$ mm/min with a constant brushing depth $d = 0.5$ mm (variant 2 ÷ 6). In the second stage of the research, the brushing depth was increased for variants 2 and 6 (the depth was increased by 0.1 mm, introducing the designations 2A and 6A). Taking into account the lowest value of the Sa parameter for variant no. 6, in the next step, for the feed rate $f = 120$ mm/min, the depth was increased in steps of 0.1 mm (variant 7 ÷ 9). The Figure 2b shows the selected section of welded joints after brushing. All variant was presented in Table 1.

Residual stress analysis was performed by X-ray diffraction using a Proto iXRD Combo and computer software XRD Win 2.0 by Proto Manufacturing. For calculate the values of residual stresses at a given measurement point was used the $\sin 2\Psi$ method [20] with the diffraction angle ($2\theta = 139.3^\circ$) in the range within 25° to 25° . The $\sin 2\Psi$ method is based on the use of BraggBrentan symmetrical diffraction [21]. In this measurement was used lamp with a chrome anode and a beam of characteristic radiation $\text{CrK}\alpha$ with a wave length $\lambda = 2.291 \text{ \AA}$ with a collimator diameter of

2 mm. The anode current, and voltage were 4 mA and 20 kV, respectively. The values of Poisson's ratio and Young's modulus were $\nu = 0.33$ and $E = 73.1 \text{ GPa}$ [22], respectively. The measurements were made in transverse direction on a weld area before and after brushing.

Surface roughness was measured with using the optical profilometer Talysurf CCI Lite. The measurements were carried out according to EN ISO 4287:1999 [23]. The joints were measured with triple repetition. Next, selected amplitude parameters and surface topography were analyzed.

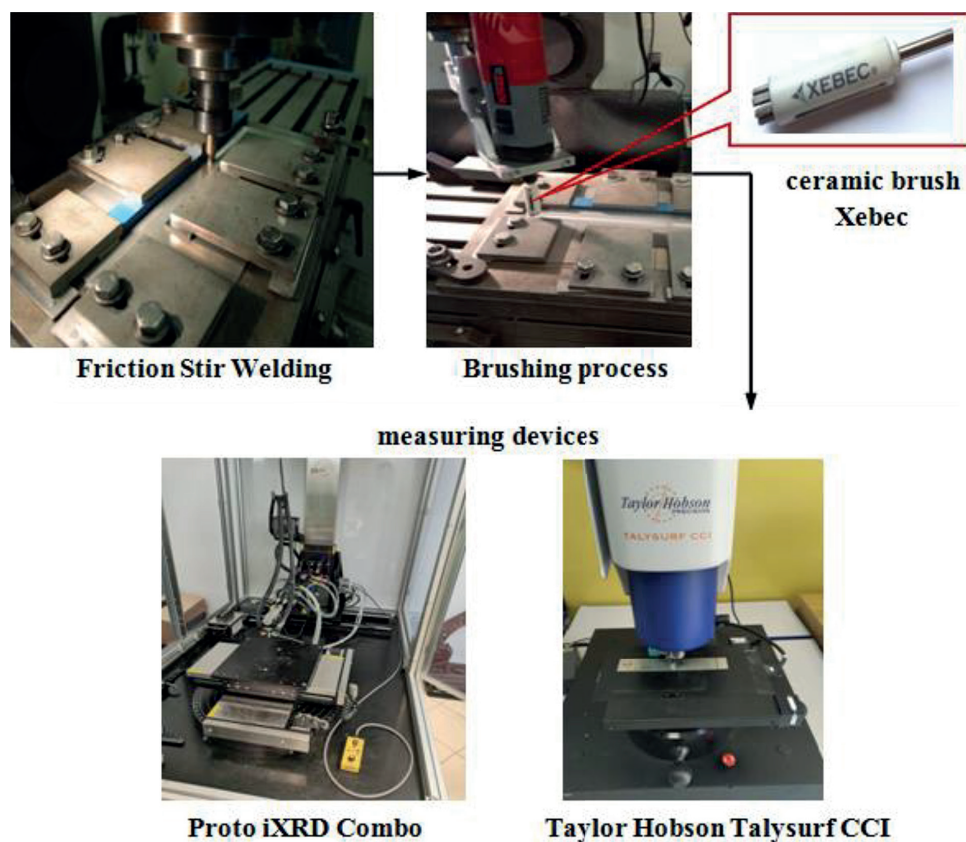


Fig. 1. Experimental setup

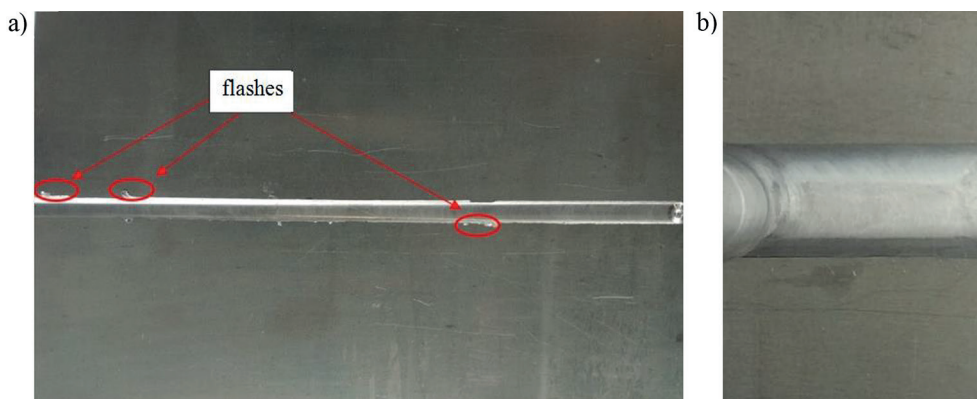


Fig. 2. Sheets after: (a) FSW method, (b) brushing

Table 1. Parameters of the experimental tests

Treatment variant	Feed rate <i>f</i> , mm/min	Brushing depth <i>d</i> , mm
1*	-	-
2	40	0.5
3	60	0.5
4	80	0.5
5	100	0.5
6	120	0.5
2A	40	0.6 (0.5+0.1)
6A	120	0.6 (0.5+0.1)
7	120	0.7 (0.5+0.2)
8	120	0.8 (0.5+0.3)
9	120	0.9 (0.5+0.4)

Note: 1* – base variant, without treatment.

RESULTS AND DISCUSSION

Surface roughness

Table 2 summarizes the results of commonly used the roughness parameters. The surface roughness parameters considered in this work were: *Sa* (arithmetical mean of the height deviations of the surface), *Sq* (root mean square height of the surface), *Sz* (the maximum height of surface), *Ssk* (skewness of height distribution) and *Sku* (kurtosis of height distribution).

Brushing welded joints made of the Al 2024-T3 alloy had a positive effect on the reduction of roughness parameters (Table 2). In this research, the *Sq* parameter is strongly correlated with *Sa* parameter. The Pearson correlation coefficient is $r = 0.99$. Therefore, the further part of the analysis focuses on one of these parameters (*Sa*) most often used in practice. In the first stage of the research, the arithmetical mean of the height deviations in the surface decreased from $Sa = 5.285 \mu\text{m}$ for joints after welding (variant 1) to $Sa = 2.460 \mu\text{m}$ for $f = 120 \text{ mm/min}$ and $d = 0.5 \text{ mm}$ (variant 6), which corresponds to a decrease of 53%. A similar relationship was observed for the parameter *Sz*, a decrease in the value of *Sz* in the range of 45÷51% can be noticed. At this stage of the research (variant 2÷6), no linear relationship between the feed rate *f* and the value of the *Sa* and *Sz* parameters can be noticed. Therefore, in the next stage, the influence of the brushing depth on the surface roughness parameters was analyzed. The lowest value of the parameter $Sa = 0.443 \mu\text{m}$ and $Sz = 3.140 \mu\text{m}$ was obtained for the brushing depth $d = 0.6 \text{ mm}$ and $f = 120 \text{ mm/min}$ (variant 6A), which is a decrease

Table 2. Results of surface roughness

Treatment variant	<i>Sa</i> , μm	<i>Sq</i> , μm	<i>Sz</i> , μm	<i>Ssk</i>	<i>Sku</i>
1*	5.285	6.490	30.700	-0.725	9.640
2	3.300	3.975	16.900	-0.651	4.910
3	2.665	3.395	16.200	-0.870	3.875
4	3.035	3.700	16.250	-1.043	3.280
5	3.415	4.110	16.450	-0.988	3.810
6	2.460	3.135	15.100	-1.235	4.020
2A	1.030	1.340	8.680	-0.380	4.850
6A	0.443	0.555	3.140	0.289	3.670
7	0.651	0.826	4.790	-0.263	3.400
8	1.100	1.430	8.100	-0.868	4.570
9	1.380	1.730	8.480	-0.271	3.380

by 92% and 90%, respectively, compared to variant 1. Pearson correlation coefficient between the brushing depth and the *Sa* and *Sz* parameters is respectively $r = 0.99$ and $r = 0.96$ (for $f = 120 \text{ mm/min}$). The *Sku* parameter is usually presented together with the *Ssk*, describing the shape of a topographic surface and its roughness distribution. Mathematically, the skewness and kurtosis parameters measure the symmetry and histogram deviation of all peaks and valleys heights of the treated surface with respect to the Gaussian distribution. A surface with a Gaussian distribution, which is symmetrically distributed, has the $Ssk = 0$. Positive *Ssk* values indicate the predominance of high peaks in turn negative values indicate the prevalence of valleys. In turn, *Sku* parameter measures the degree of flattening or thinning of a topographic distribution of a peak's roughness profile. On a surface with normal symmetric distribution, the *Sku* being 3. In practical terms, *Sku* being greater than 3 indicates the presence of acute peaks, while *Sku* is less than 3 indicates surface texture free of disproportionately sharp peaks [24]. In this work, only for the variant 6A skewness is positive $Ssk = 0.289$. For rest variants the parameter *Ssk* is negative. The minimum value of skewness occurred in variant 6 (-1.235). As for the *Sku* parameter, the minimum and maximum results are respectively found in variant 4 (3.280) and variant after FSW no. 1 (9.640). Therefore, it can be concluded that brushing the welded joints with the feed rate $f = 120 \text{ mm/min}$ and the depth $d = 0.6 \text{ mm}$ (variant 6A) flattened and rounded sharp peaks. Figure 3a presents the isometric surfaces and contour maps of the tests for the surface after FSW treatment. The surface topography map shows typical traces of the tool after friction stir welding. In turn, Figure 3b

shows the surface topography after brushing with a Xebec ceramic brush. As a result of brushing, a new roughness structure was formed, on which the high peaks after the previous process were reduced, which is also confirmed by the presented roughness profiles.

Residual stress

Table 3 presented the results of the residual stress for all variants with measurement error. The change of the feed speed in the range of 40÷120 mm/min did not significantly affect the

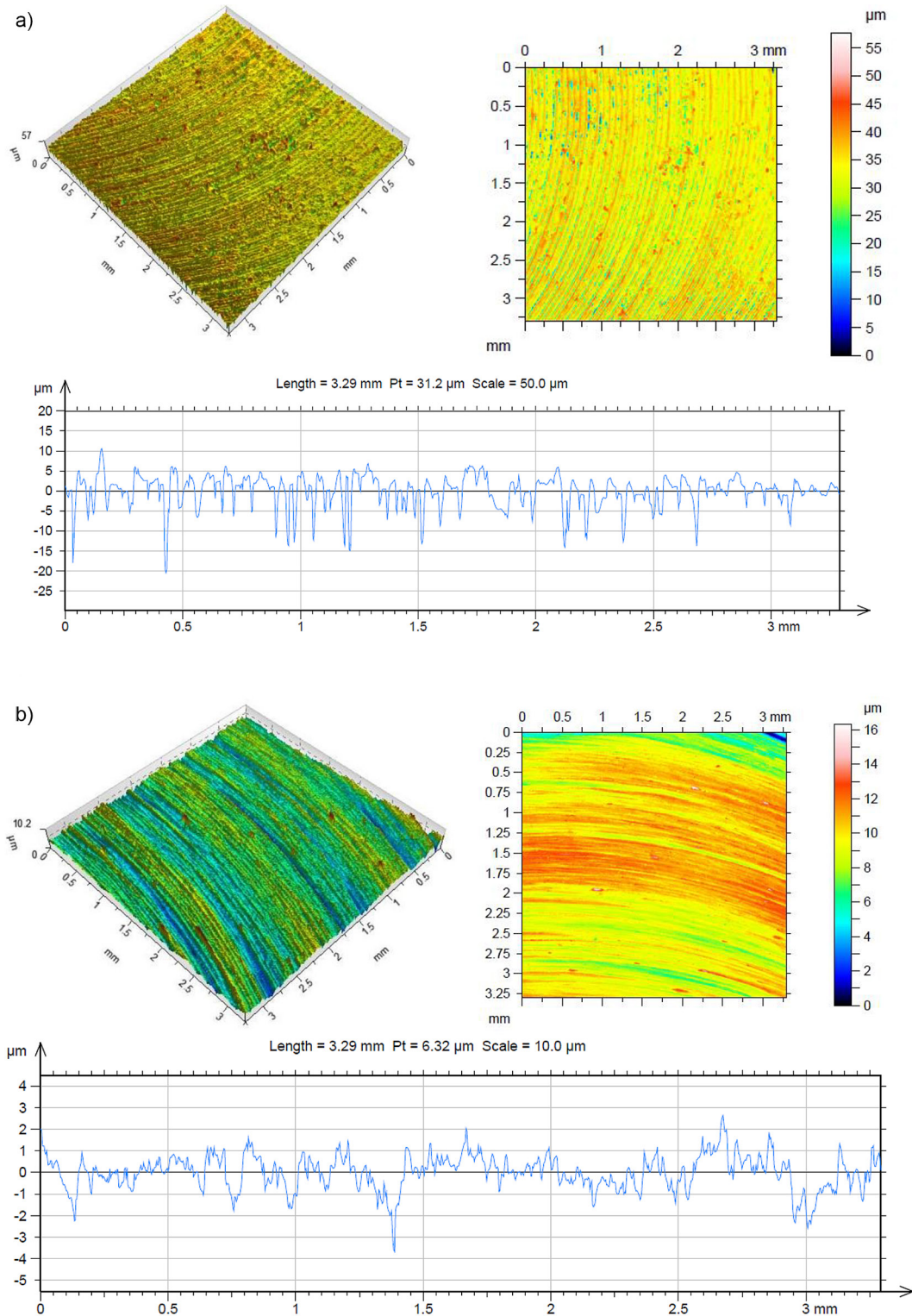


Fig. 3. Surface topography. Isometric views, contour maps and roughness profiles after: (a) FSW method, (b) brushing $f = 120$ mm/min, $d = 0.6$ mm

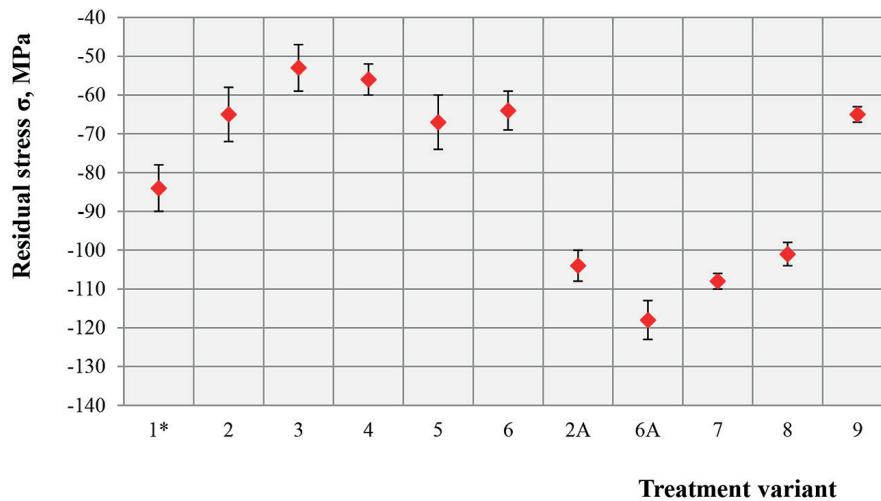


Fig. 4. Residual stress of the EN AW-2024-T3 welded joints after brushing

value of compressive stresses for variants 2 ÷ 6. It amounts to $\sigma = -67 \div -53$ MPa, the difference, however, is within the error limits of the measurements. A significant difference can be observed in the second stage of the research. The highest value of compressive stresses $\sigma = -118$ MPa was obtained for $f = 120$ mm/min and $d = 0.6$ mm, which is an increase of 40.5% compared to the sample after FSW. For the feed speed $f = 120$ mm/min, it can be seen that with the increase of brushing depth, the value of compressive stresses decreases (variant 6A ÷ 9). Brushing depth $d = 0.9$ mm (variant 9) introduces stresses of the order of $\sigma = -65$ MPa ± 2 MPa, which in turn are comparable to brushing for the feed speed in the range $f = 40 \div 120$ mm/min and depth $d = 0.5$ mm. Hence, in further research, this variant should be rejected, if only because of the faster wear of the tool.

The analysis of the obtained test results showed, that for the feed rate $f = 120$ mm/min, the roughness parameter Sa is strongly correlated with the residual stresses σ (Fig. 5). The value of Pearson’s correlation coefficient is $r = 0.87$.

CONCLUSIONS

The paper presents the selection of parameters for the brushing process of FSW welded joints made of the aluminum alloy EN AW-2024-T3. The influence of selected process parameters (feed rate and brushing depth) on the surface topography and residual stresses was also analyzed. Based on the experimental results, the following important conclusions were drawn. Brushing with a depth of $d = 0.5$ mm with a feed speed in the range $f = 40 \div 120$ mm/min decreased the value of the Sa parameter in the range from 35.4% to

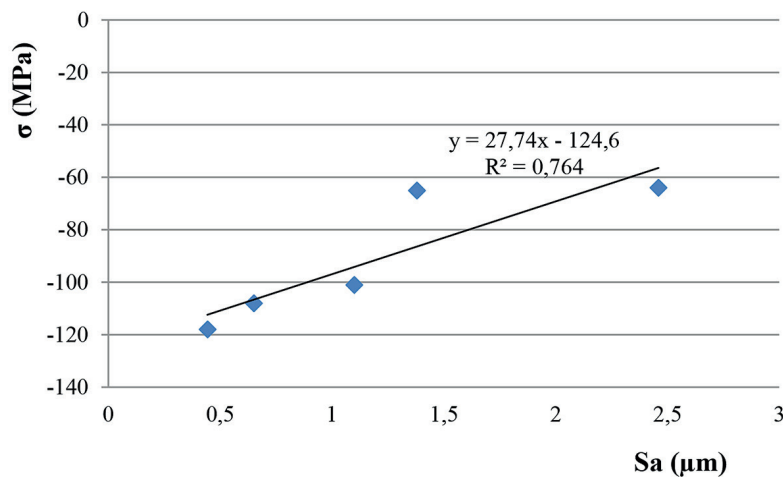


Fig. 5. Graph of the correlation of the Sa and σ for feed speed $f = 120$ mm/min

53.5% compared to the specimen after FSW. The smallest surface roughness $Sa = 0.443 \mu\text{m}$ and $Sz = 3.140 \mu\text{m}$ and the highest compressive stresses $\sigma = -118 \text{ MPa}$ were obtained for the feed speed $f = 120 \text{ mm/min}$ and depth $d = 0.6 \text{ mm}$. Therefore, it can be concluded that these parameters are optimal in the adopted scope of research. The value of the Pearson correlation coefficient $r = 0.87$ for the Sa parameter and residual stresses proves a large dependence of these parameters (for variants 6A÷9). As compressive stresses increase, the roughness value decreases. The brushing treatment has a positive effect on the condition of the surface layer of the joints after FSW welding and eliminates the burs formed during the welding process.

Acknowledgments

This work was supported by Polish National Agency for Academic Exchange, project title: „Research into innovative forming and joining methods of thin-walled components”, project number: BPN/BSK/2021/1/00067/U/00001.

REFERENCES

- Smallbone C., Kocak M. Improving global quality of life through optimum use and innovation of welding and joining technologies, Cedex: International Institute of Welding, 2012.
- Storjohann D., Barabash O.M., David S.A. et al. Fusion and friction stir welding of aluminum-matrix composites. *Metallurgical Materials Transactions A* 2005; 36(11): 3237–3247. <https://doi.org/10.1007/s11661-005-0093-4>
- Shah S., Tosunoglu S. Friction Stir Welding: Current State of the Art and Future Prospects. *Material Science The 16th World Multi-Conference on Systemics, Cybernetics and Informatics, Orlando, Florida* 2012; 17–20.
- Bucior M., Kluz R., Kubit A., Ochał K. Analysis of the Possibilities of Improving the Selected Properties Surface Layer of Butt Joints Made Using the FSW Method. *Advances in Science and Technology Research Journal* 2020; 14(1): 1–9. <https://doi.org/10.12913/22998624/111662>
- Thakur A., Sharma V., Bhadauria S.S. Investigation of metallurgical characterization and mechanical properties of double-sided friction stir welding of aluminum 6061 T6 alloy. *Proceedings of the Institution of Mechanical Engineers, Part B: Journal of Engineering Manufacture*. April 2022. <https://doi.org/10.1177/09.544054221092935a>.
- Forsström A., Bossuyt S., Yagodzinsky Y., Tsuzaki K., Hänninen H. Strain localization in copper canister FSW welds for spent nuclear fuel disposal. *Journal of Nuclear Materials* 2019; 532: 347–359. <https://doi.org/10.1016/j.jnucmat.2019.06.024>
- Mira-Aguiar T., Verdera D., Leitão C., Rodrigues D.M. Tool assisted friction welding: A FSW related technique for the linear lap welding of very thin steel plates. *Journal of Materials Processing Technology* 2016; 238: 73–80. <https://doi.org/10.1016/j.jmatprotec.2016.07.006>
- Muhamad M.R., Jamaludin M.F., Yusof F., Mahmoodian R., Morisada Y., Suga T., Fujii H. Effects of Al-Ni powder addition on dissimilar friction stir welding between AA7075-T6 and 304 L. *Materials Science & Engineering Technology* 2020; 51(9): 1274–1284. <https://doi.org/10.1002/mawe.201900105>.
- Jabraeili R., Jafarian H. R., Khajeh R., Park N., Kim Y., Heidarzadeh A., Eivani A. R. Effect of FSW process parameters on microstructure and mechanical properties of the dissimilar AA2024 Al alloy and 304 stainless steel joints. *Materials Science and Engineering: A* 2021; 814: 140981. <https://doi.org/10.1016/j.msea.2021.140981>
- Zhang W., Shen Y., Yan Y., Guo R., Guan W., Guo G. Microstructure characterization and mechanical behavior of dissimilar friction stir welded Al/Cu couple with different joint configurations. *The International Journal of Advanced Manufacturing Technology* 2018; 94: 1021–1030. <https://doi.org/10.1007/s00170-017-0961-2>
- Aliha M.R.M., Kalantari M.H., Ghoreishi S.M.N., Torabi A.R., Etesam S. Mixed mode I/II crack growth investigation for bi-metal FSW aluminum alloy AA7075-T6/pure copper joints. *Theoretical and Applied Fracture Mechanics* 2019; 103: 102243. <https://doi.org/10.1016/j.tafmec.2019.102243>.
- Shehabeldeen T.A., Yin Y., Ji X., Shen X., Zhang Z., Zhou J. Investigation of the microstructure, mechanical properties and fracture mechanisms of dissimilar friction stir welded aluminium/titanium joints. *Journal of Materials Research and Technology* 2021; 11: 507–518. <https://doi.org/10.1016/j.jmrt.2021.01.026>.
- Shankar S., Chattopadhyaya S., Mehta K. P., Vilaça P. Influence of copper plate positioning, zero tool offset, and bed conditions in friction stir welding of dissimilar Al-Cu alloys with different thicknesses. *CIRP Journal of Manufacturing Science and Technology* 2022; 38: 73–83. <https://doi.org/10.1016/j.cirpj.2022.04.001>.
- Venkat Ramana G., Yelamasetti B., Vishnu Vardhan T. Effect of FSW process parameters and tool profile on mechanical properties of AA 5082 and AA 6061 welds. *Materials Today: Proceedings*

- 2021; 46: 826–830. <https://doi.org/10.1016/j.matpr.2020.12.801>.
15. Salacinski T., Chmielewski T., Winiarski M., Cacko R., Swiercz R. Roughness of Metal Surface after Finishing using Ceramic Brush Tools. *Advances in Materials Science* 2018; 18(55): 20–27. <https://doi.org/10.1515/adms-2017-0024>
 16. Matuszak J. Effect of ceramic brush treatment on the surface quality and edge condition of aluminium alloy after abrasive waterjet machining. *Advances in Science and Technology Research Journal* 2021; 15(3): 254–263. <https://doi.org/10.12913/22998624/140336>
 17. Matuszak J., Klonica M., Zagorski I. Effect of Brushing Conditions on Axial Forces in Ceramic Brush Surface Treatment. In *Proceedings of the 2019 IEEE 5-th International Workshop on Metrology for AeroSpace (MetroAero Space)*; IEEE: Torino, Italy 2019, 644–648.
 18. Robitaille B., Provencher P.R., St-Georges L., Brochu M. Mechanical properties of 2024-T3 Al-Clad aluminum FSW lap joints and impact of surface preparation. *International Journal of Fatigue* 2021; 143: 105979. <https://doi.org/10.1016/j.ijfatigue.2020.105979>.
 19. ASTM B209M-Standard Specification for Aluminum and Aluminum-Alloy Sheet and Plate; ASTM International: West Conshohocken, (2014) PA, USA.
 20. Bonarski J.T. Measurement and use of the texture stress microstructure characteristics in materials diagnostics. Institute of Metallurgy and Materials Science of the Polish Academy of Sciences. Cracow, 2013. (in Polish)
 21. Skrzypek S.J. New possibilities of measuring macro stress of materials using X-ray diffraction in the geometry of a constant angle of incidence. Publisher AGH. Cracow 2002. (in Polish)
 22. Kłysz S. Basics of strength of materials. Publisher: Technical Institute of Air Forces. Warsaw 2015. (in Polish)
 23. EN ISO 4287: 1999. Geometrical product specifications (GPS). Surface texture: Profile method. Terms, definitions and surface texture parameters.
 24. Dong W.P., Sullivan P.J., Stout K.J. Comprehensive study of parameters for characterizing three-dimensional surface topography III: Parameters for characterizing amplitude and some functional properties. *Wear* 1994; 178: 29–43. [https://doi.org/10.1016/0043-1648\(94\)90127-9](https://doi.org/10.1016/0043-1648(94)90127-9)